ISSN 1070-3284, Russian Journal of Coordination Chemistry, 2022, Vol. 48, No. 12, pp. 839–845. © Pleiades Publishing, Ltd., 2022.

New Ferrocenemethylated Salan $[H_2(MeFc)_2]$-Salan Ligand and Its Pd(II) Complex: Synthesis and Crystal Structure

B. Anzaldo[a], P. Sharma[a], *, **, C. P. Villamizar[a], R. González[a], R. Gutiérrez Pérez[b], and Abiram Rosas[b]

[a] *Instituto de Química Universidad Autónoma de México UNAM, Cd., Universitaria, Ciudad de México, PO Box 04510 México*

[b] *Lab. Síntesis de Complejos, Fac. Cs. Quím.-BUAP, Ciudad Universitaria, Puebla, PO Box 72592 México*

**e-mail: pankajsh@unam.mx*

***e-mail: jrgutie@correo.buap.mx*

Received February 26, 2022; revised March 16, 2022; accepted April 14, 2022

Abstract—The synthesis of a new ferrocenemethylated salan $[H_2(MeFc)_2]$-salan ligand (L) and its palladium complex $[Pd^{II}(MeFc)_2]$-salan (**I**) is described. The ligand and its complex **I** were characterized by ^1H, $^{13}C\{^1H\}$ 2D-NMR techniques, IR spectroscopy and mass spectrometry. X-ray crystal structure of ligand L has been determined (CCDC no. 1557925), which crystalizes in monoclinic ($P2_1/n$) symmetry and displays intramolecular OH···N hydrogen bonding.

Keywords: ferrocenemethyl Pd complex, salan ligand, N and O donors

DOI: 10.1134/S1070328422100128

INTRODUCTION

The multidentate ligands containing N and O donor atoms are used to obtain coordination complexes [1, 2] with wide applications in different branches of chemistry. Some of the common ligands with these donor atoms are: picolinic acid [3, 4]. 8-Hydroxyquinoline [5], ethylenediamine-*N*,*N*-diacetate (Edda) [6] and different Schiff bases. Particularly, 1,2-bis(salicylaldiminato)ethane ($[H_2]$-salen) is one of the most widely studied ligands in the coordination chemistry because the ligand contains potentially O, N, N, O donor atoms and commonly act as a tetradentate ligand. In general, multidentate Schiff base ligands are cheap, facile to synthesize, and can be easily modulated with different steric and electronic properties [7–9].

The reduced form of in H_2salen type ligand, which is known as $[H_4]$-salan should also be useful in the formation of complexes but have been explored lesser. However these ligands not only offer greater flexibility than the $[H_2]$-salen but further possess two additional sites capable of bonding with metal in a higher oxidation state [10, 11]. The different hybridization of the nitrogen atoms in $[H_2]$-salen and $[H_4]$-salan ligands may differentiate in the formation of the corresponding complexes in a substantial way as amine nitrogen has higher donor ability.

On the other side ferrocene-based salen and salan ligands and their metal complexes have not been explored much [12, 13]. The presence of ferrocene motif provides different steric and electronic properties because of its rigidity and donating ability. Taking this in consideration and scarcity of reports where both the nitrogen atoms are tertiary amine nitrogen, this work was undertaken. This report presents the synthesis and characterization of new $[H_2]$-salan and its palladium(II) complex.

EXPERIMENTAL

Materials and apparatus. The material was acquired from Sigma-Aldrich and Strem Chemicals and employed without any further purification: *N*,*N*-Dimethylaminomethylferrocene, methyl iodide, $Pd(OCOCH_3)_2$, K_2CO_3, Analytical thin layer chromatography (TLC) was performed using silica gel plates ($60GF_{254}$). The developed chromatogram was analyzed by UV lamp (254 nm). The silica gel column chromatography was performed with 70–230 and 230–400 mesh. Melting points (mp) were determined using a Mel-Temp Melting Point apparatus. Infrared (IR) spectra were recorded on a Bruker Alpha-P FTIR spectrophotometer with an attenuated total reflectance (ATR) technique. The ^1H and ^{13}C NMR spectra were recorded on a Bruker Avance™ 300 MHz, in $CDCl_3$ using TMS as an internal standard. Chemical shift values are reported in parts per million (δ, ppm) and *J* values are in Hertz. The splitting pattern are indicated as follows abbreviations: singlet (s.), doublet (d.), doublet of doublet (d.d.), triplet (t.), quartet (q.) and multiplet (m). High-resolution mass spectrometry (HRMS) was recorded on a Jeol AccuTOF JMS-

T100LC mass spectrometer. The FAB^+ technique used in mass spectrometry with matrix of 3-nitrobenzyl alcohol (3-NOBA).

Synthesis of $[H_2(MeFc)_2]$-salan (L). To a stirred solution of (trimethylaminomethyl) ferrocene iodide $(Cp)Fe[(Me_3N^+CH_2)C_5H_3][I^-]$ 1.80 g (2.42 mmol) in acetonitrile (30 mL) and K_2CO_3 (4.8 mmol) was added *N*,*N*'-bis(2-hydroxybenzyl)ethylenediamine 0.300 g (1.10 mmol) at room temperature. The mixture was stirred at reflux temperature for 24 h. The reaction mixture after cooling to room temperature was concentrated at reduced pressure and the product was isolated by column chromatography using silica gel with ratio 1:1 n-hexane: ethyl acetate. The ligand L was isolated in good yield ~80% and stable to air. Melting point: 140°C. ^1H NMR ($CDCl_3$; 300 MHz; δ, ppm): 1.50 (2H, s., H-13), 2.57 (4H, s., H-14), 3.45 (4H, s., H-5), 3.62 (4H, s., H-6), 4.03 (10H, s., H-4), 4.08–3.95 (4H, m., H-3), 4.19–4.07(4H, m., H-2), 6.97–6.74 (6H, m., H-9, H-10, H-11), 7.20 (2H, t.d. ($J_{H-H.}$=.7.8,1.07), H-8), ^{13}C NMR ({^1H}, $CDCl_3$; 75 MHz; δ, ppm): 49.43 (C-14), 52.26 (C-6), 57.36 (C-5), 68.52 (C-3), 68.55 (C-4), 70.24 (C-2), 80.01 (C-1), 116.14 (C-9), 119.26 (C-11), 121.90 (C-7), 128.75 (C-10), 157.79 (C-4). DART-MS *m/z*: 669 [M + H].

Synthesis of $[Pd^{II}(MeFc)_2]$-salan (I). Ligand L (0.2 g, 0.3 mmol) was dissolved in 20 mL of MeOH and the solution was added to $[Pd(OAc)_2]$ (0.0673 g, 0.3 mmol) in 2 mL MeOH. The mixture was refluxed for 2 h.

Synthesis of $[H_2(MeFc)_2]$-salan (L) and its complex (I) was illustrated in Scheme 1.

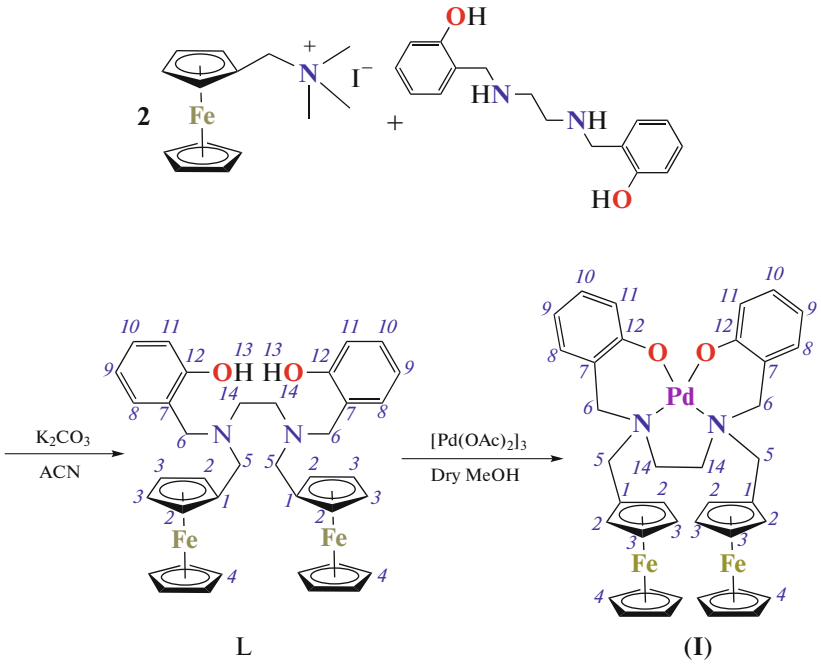

L (I)

Scheme 1.

The product was isolated with silica gel by column chromatography, using ethyl acetate as eluent, was obtained in a moderate yield 42%. Melting point: 132°C, ^1H NMR ($CDCl_3$, 300 MHz, δ, ppm): 2.56 (4H, d.d., J_{H-H} = 64.69, 9.02, H-14), 3.10 (2H, d., J_{H-H} = 13.5, H-16), 3.47 (2H, d., J_{H-H} = 14.02, H-5), 3.97 (10H, s., H-4), 4.03 (10H, s., H-4), 4.01–3.99 (2H, m., H-3), 4.12–4.09 (2H, m., H-3), 4.14 (2H, d., J_{H-H} = 14.1, H-5), 4.21–4.18 (2H, m., H-2), 4.29 (2H, d., J_{H-H} = 13.4, H-6), 4.82–4.55 (2H, m., H-25), 6.42 (2H, t.t., J_{H-H} = 7.0, 1.6, H-8), 6.73 (2H, d.d., J_{H-H} = 7.5,1.7, H-9), 7.13–6.85 (4H, m., H-11, H-10), ^{13}C NMR ({^1H}, $CDCl_3$; 75 MHz; δ, ppm): 55.56 (C-6), 57.47 (C-14), 63.78 (C-5), 69.03 (C-4), 69.37 (C-3), 69.61 (C-3), 70.84 (C-2), 71.73 (C-2), 76.87 (C-1), 113.70 (C-8), 118.98 (C-7), 120.56(C-10), 129.57 (C-9), 130.07 (C-11), 162.78 (C-H-12). FAB^+ MS *m/z*: 773 [M + H]. HRMS (FAB): Found 773.0746, calcd. for $C_{38}H_{39}N_2O_2Fe_2Pd$ $[M + H]^+$ 773.0745.

X-ray structure determination. The diffraction intensity data of **I** were collected on Bruker Smart APEX diffractometer using graphite monochromated MoK_α radiation (λ = 0.71073 Å). Data reduction was carried out with the SAINT software [14]. The structure was solved by direct methods and refined by full-matrix least-squares methods based on F^2 using SHELXS-2012 program. Nonhydrogen atoms were

Table 1. Crystallographic data and structure refinement information for L

Parameter	Value
Empirical formula	$C_{38}H_{40}N_2O_2Fe_2$
Mr	668.42
Crystal system, space group	Monoclinic, $P2_1/n$
Temperature, K	298
a, Å	10.988(2)
b, Å	10.049(2)
c, Å	14.601β(3)
β, deg	104.491(5)
V, Å^3	1560.8(6)
Z	2
μ, mm^{-1}	0.97
Crystal size, mm	0.48 × 0.16 × 0.07
Absorption correction	Multi-scan (Sheldrick, 2008)
T_{min}, T_{max}	0.470, 0.877
Reflections measured, independent and observed ($I > 2\sigma(I)$)	15207, 3438, 2351
R_{int}	0.052
sin θ/λ_{max}, Å^{-1}	0.641
R ($F^2 > 2\sigma(F^2)$), $wR(F^2)$, S	0.041, 0.103, 1.03
No. of reflections	3438
No. of parameters	248
No. of restraints	186
H-atom treatment	H atoms treated by a mixture of independent and constrained refinement
$\Delta\rho_{max}$, $\Delta\rho_{min}$, e Å^{-3}	0.25, −0.25

refined anisotropically. H atoms were positioned geometrically and refined with isotropic displacement parameters according to the riding model SHELXL-2014/7 program [15]. The crystallographic data are presented in Table 1.

The supplementary crystallographic data of the ligand (L) has been deposited with the Cambridge Crystallographic Data Center (CCDC no. 1557925; http://www.ccdc.cam.ac.uk/data_request/cif).

RESULTS AND DISCUSSION

The compound L was synthesized by reacting *N*,*N*,*N*-trimethylaminomethyl ferrocene iodide (Cp)Fe[($Me_3N^+CH_2$)C_5H_3][I^-] with *N*,*N*'-bis(2-hydroxybenzyl)ethylenediamine using K_2CO_3 as a base in acetonitrile. The Pd(II)-salan complex **I** was obtained by reacting SALAN ligand L with palladium acetate as shown in Scheme 1.

In the ligand L a weak vibration at 3306 cm^{-1} was observed, which may be ascribed to O–H vibration with an intramolecular O–H···N hydrogen bonding, C–H vibration of ferrocene skeleton are observed in 800 to 1100 cm^{-1} range. IR spectra of complex **I** do not present O–H vibration confirms the coordination of oxygen to palladium center. The appearance of additional vibrations ~480 and ~520 cm^{-1} that can be ascribed to ν(Pd–O) and ν(Pd–N), respectively, further support the formation of this complex. The mass spectra show the molecular ion peak [M + H] for compounds L (Fig. 1) and molecular ion peak for complex **I** (Fig. 2).

All the signals in the ^{1}H (Table 2) and ^{13}C NMR spectra of L and complex **I** have been completely assigned using 2D: COSY, HSQC and HMBC techniques. In the proton NMR spectra of the ligand the OH-proton show a broad signal at 1.58 ppm, which disappears in ^{1}H NMR spectra of the palladium com-

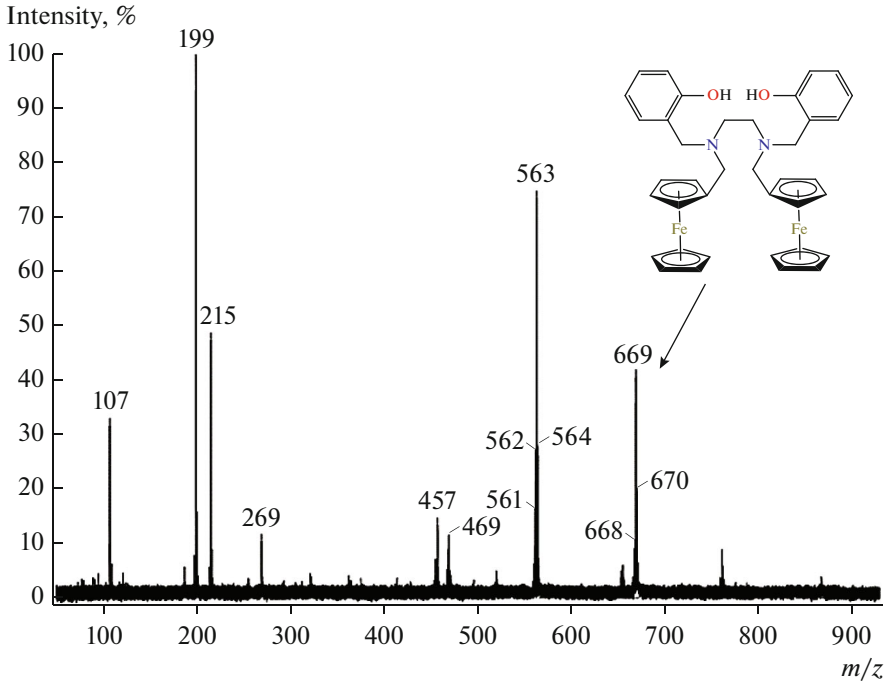

Fig. 1. Mass spectrometry DART for ligand L.

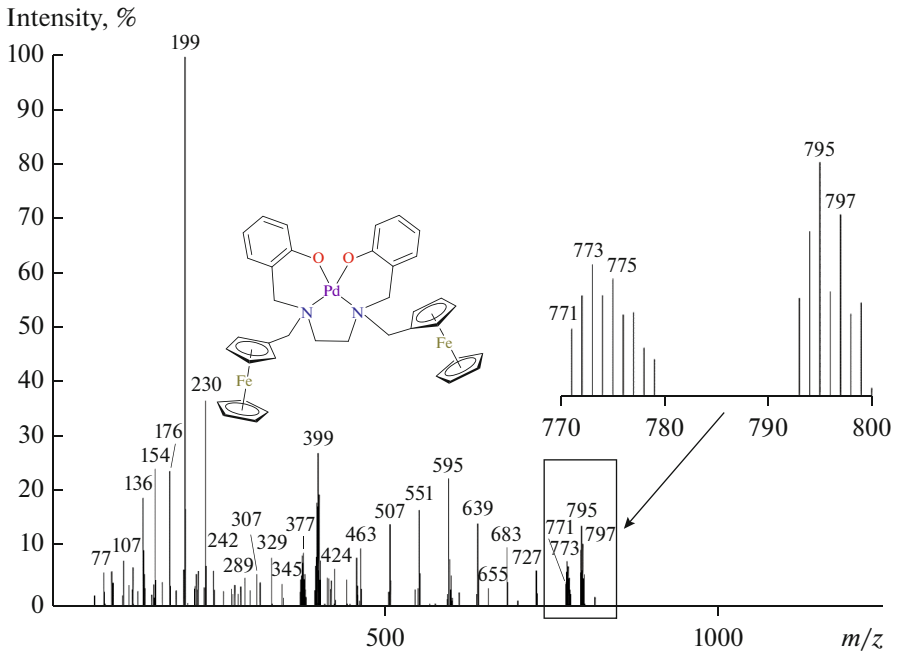

Fig. 2. Mass spectrometry of FAB^+ for complex **I**.

plex (**I**). In the ^{13}C NMR of the complex, the phenolic carbon atom shows a downfield shift of 5 ppm in comparison to the ligand, while an upfield shift of 8 ppm for $-NCH_2CH_2$ carbon was observed in the NMR spectra of the complex compared to the ligand spectra confirm the coordination of both the N,O donor sites.

The substituted cyclopentadienyl ring of ferrocene linked to CH_2N- group display four δ signals at 4.74, 4.26, 4.18, and 4.06 ppm as multiplets and similarly for the ^{13}C signals 69.37 ppm (C-3), 69.61 ppm (C-3), 70.84 ppm (C-2), 71.73 ppm (C-2) which show the nonequivalence of these protons and carbon atoms. Interestingly in the NOESY spectra NOE interactions

Table 2. NMR data of ligand L and its complex **I**

Proton	Ligand (δ, ppm)	Complex (δ, ppm)
H-14	s., 2.57	d.d., 2.56 (J_{H-H} = 64.69, 9.02)
H-5	s., 3.62	d., 3.10 (J_{H-H} = 13.4), d., 4.29 (J_{H-H} = 13.4)
H-6	s., 3.45	d., 3.47 (J_{H-H} = 14.0), d., 4.14 (J_{H-H} = 14.0)

were observed between protons H-2 of Cp substituted ring with H-5 protons in complex **I** as shown in Figs. 3a, 3b.

Furthermore, the palladium complex **I** has two N chiral centers which can give four distereomers. ^{1}H NMR spectra of palladium complex shows the presence of two diastereomers in 3 : 1 ratio. After purification by synthetic thin layer chromatography, only one diastereomer was isolated which can be either *meso* or diastereomer RR/SS.

The complex **I** crystallizes in the monoclinic system in $P2_1/n$ space group. The asymmetric unit (Fig. 4a) is half of the molecule structure (Fig. 4b) generated from a inversion center [0, 0, 0; $-x$, $-y$, $-z$], The carbon atoms of one of the cyclopentadienyl rings are disordered and the carbon atoms were refinement over two positions, the selected bond lengths and bond angles for ligand L showed in Table 3.

The influence of the steric strain caused by the organic groups and the torsion angle C(10)–C(9)–N(1)–C(1) (–73.9(2)°), compared with the C(1)–N(1)–C(8)–C(2) (65.8(3)°). The steric bulk because

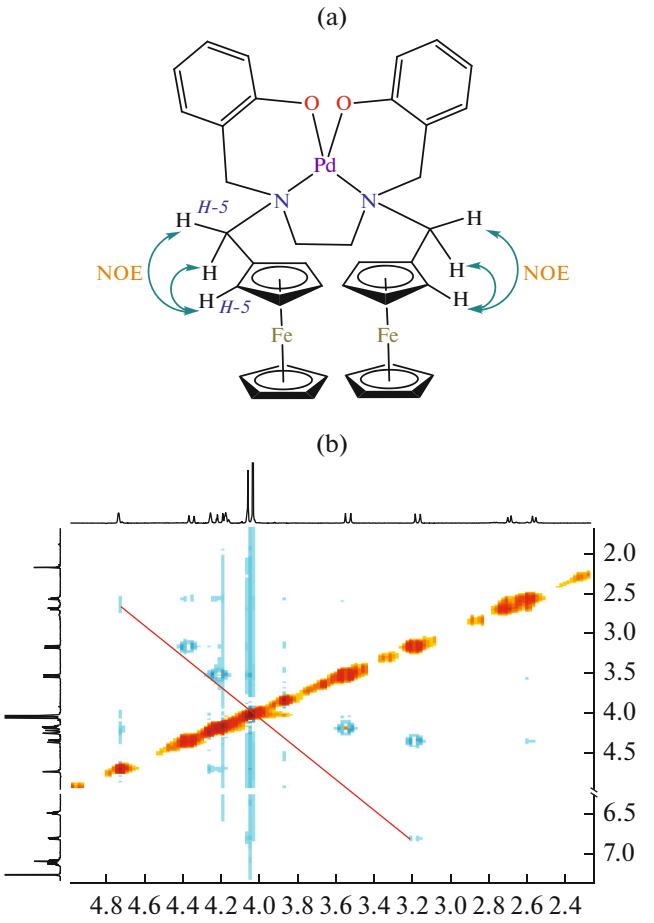

Fig. 3. NOESY interaction between H-5 and H-2 protons in complex **I**: molecular structure for complex **I** (a); NOESY NMR spectra for complex **I** (b).

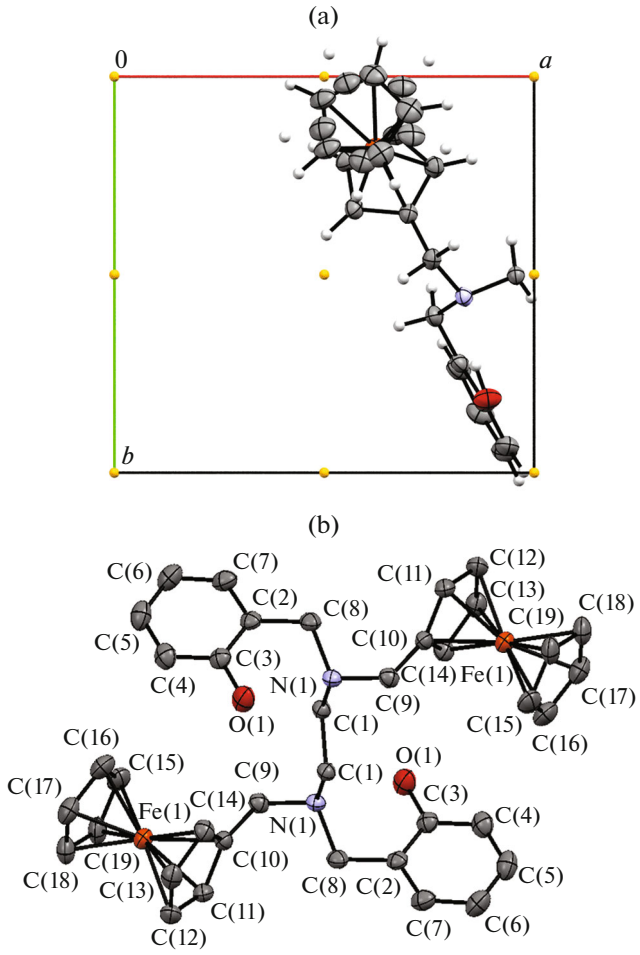

Fig. 4. Asymmetric unit for ligand and inversion center L (a); molecular structure of ligand L (b) (displacement ellipsoids at 30% probability). H atoms are removed for clarity.

Table 3. Selected bond lengths and bond angles for ligand L

Bond	*d*, Å	Bond	*d*, Å
C(10)–C(9)	1.515(3)	C(9)–N(1)	1.484(3)
N(1)–C(8)	1.468(4)	C(8)–C(2)	1.508(4)
N(1)–C(1)	1.470(3)	C(1)–C(1)	1.521(4)
Angle	ω, deg	Angle	ω, deg
C(11)C(10)C(9)	125.1(2)	C(9)N(1)C(8)	111.2(2)
C(14)C(10)C(9)	128.2(2)	N(1)C(8)C(2)	113.3(2)
C(10)C(9)N(1)	115.7(2)	C(3)C(2)C(8)	121.2(2)
N(1)C(1)C(1)	110.9(2)	C(8)N(1)C(1)	111.9(2)
C(1)N(1)C(9)	113.2(2)	C(7)C()C(8)	120.7(2)

of the presence of ferrocenemethyl also affect the planarity with atom N(1) deviating by 49.32° from the plane in which they are attached: C(2)–C(8)–N(1) and plane in Cp group plane: C(10)–C(9)–N(1).

A packing diagram of the ligand L is presented in Fig. 5 which shows that the intramolecular hydrogen-bonding interaction O–H···N (1.84(3) Å) was observed that affords its packing into supramolecular layers along with the structure with (2-fold) screw axis with direction [0, 1, 0], furthermore, a glide plane perpendicular to [0, 1, 0].

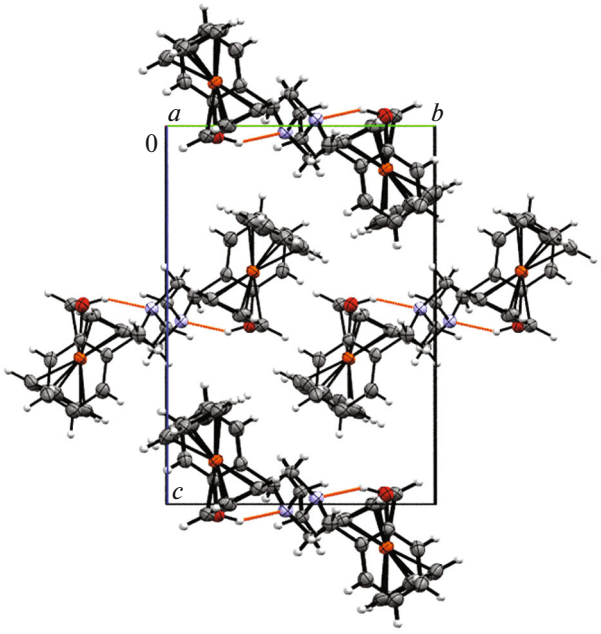

Fig. 5. The packing arrangement in the crystal of ligand L. A dashed line indicates the intramolecular hydrogen bond bridges by O–H···N.

Then, new ferrocenemethylated-salan $[H_2(MeFc)_2]$-salan ligand L and its palladium complex $[Pd^{II}(MeFc)_2]$-salan (**I**) have been synthesized. The ligand and its palladium complex **I** are characterized by ^1H and ^{13}C NMR, NOESY, IR spectroscopy and mass spectrometry. X-ray crystal structure of the ligand L has been determined, which crystalizes in monoclinic ($P2_1/n$) system and displays intramolecular OH ···N hydrogen bonding interaction (1.84 (3) Å) that affords its packing into supramolecular layers along with the structure.

ACKNOWLEDGMENTS

We thank Dr Toscano for solving the crystal structure and to DGAPA, UNAM, Mexico (IN209020) for the financial support and CONACyT (Fellowship 368610).

CONFLICT OF INTEREST

The authors declare that they have no conflicts of interest.

SUPPLEMENTARY INFORMATION

The online version contains supplementary material available at https://doi.org/10.1134/S1070328422100128.

REFERENCES

1. Schnaars, K., Kaneko, M., and Fujisawa, K., *Inorg. Chem.*, 2021, vol. 60, p. 2477.
2. Shah, S.R., Shah, Z., Khiat, M., et al., *ACS Omega*, 2020, vol. 5, p. 10200.
3. Aizawa, S.I., Natsume, T., Hatano, K., and Funahashi, S., *Inorg., Chim. Acta*, 1996, vol. 248, p. 215.
4. Jeon, J.Y., Lee, J.J., Varghese, J.K., et al., *Dalton Trans.*, 2013, vol. 42, p. 9245.

5. Li, L.H., Feng, X.L., Cui, X.H., et al., *J. Am. Chem. Soc.*, 2017, vol. 139, p. 6042.
6. Zhao, X., Zhang, D., Yu, R., et al., *Eur. J. Inorg. Chem.*, 2018, vol. 2018, p. 1185.
7. Pessoa, J.C. and Correia, I., *Coord. Chem. Rev.*, 2019, vol. 388, p. 227.
8. Cozzolino, M., Leo, V., Tedesco, C., et al., *Dalton Trans.*, 2018, vol. 47, p. 13229.
9. May, N.V. Bonczidai-Kelemen, D., et al., *Inorg. Chem.*, 2021, vol. 60, p. 11259.
10. Liu, B., Chai, J., Feng, S., and Yang, B., *Spectrochim. Acta, A*, 2015, vol. 140, p. 437.
11. Wölfle, H., Kopacka, H., Wurst, K., et al., *J. Organomet. Chem.*, 2006, vol. 691, p. 1197.
12. Shafir, A., Fiedler, D., and Arnold, *Dalton Trans.*, 2002, p. 555.
13. Atkinson, R.C.J., Gerry, K., Gibson, V.C., et al., *Organometallics*, 2007, vol. 26, p. 316.
14. *APEX2, SAINT, SADABS and TWINABS*, Madison: Bruker AXS Inc., 2012.
15. Sheldrick, G.M., *Acta Crystallogr., Sect. C: Struct. Chem.*, 2015, vol. 71, p. 3.